LATERAL AUTOPILOT DESIGN FOR A UAV USING COEFFICIENT DIAGRAM METHOD

Rui Hirokawa, Koichi Sato
Mitsubishi Electric Kamakura Works

Keywords: *Flight Control Systems,Unmanned Air Vehicles, Coefficient Diagram Method*

Abstract

The lateral autopilot of an UAV is designed using Coefficient Diagram Method (CDM). The CDM is an algebraic control system design approach and the design is performed by the coefficient diagram drawing the coefficient of system characteristic polynomial. The lateral control system is formulated as MIMO system and is divided into beta and bank control problems by control input decoupling. The controllers are successfully designed by CDM and the performance is confirmed by six-degrees-of-freedom (6DOF) simulation.

1 Introduction

By the recent advance of MEMS sensors and GPS technologies, the low-cost miniature UAV have become realisable. The flight controller of such UAV is required to be simple and robust because of the CPU resource restriction of the onboard micro-controller. In this paper, the lateral autopilot of an UAV having simple structure and robustness is designed using Coefficient Diagram Method (CDM). The CDM is an argebraic design approach for control system proposed by Shunji Manabe and the design is performed by the coefficient diagram drawn the coefficient of system characteristic polynomial [8]. The stability criteria of CDM is based on Lipatov's paper [4], it is represented in the coefficient diagram.

The CDM is successfully applied to the various applications such as attitude control of satellite [6] and robotic manipulator [1]. The CDM is very effective design approach for SISO systems. Recently the CDM is also applied to MIMO systems. Manabe proposed the MIMO controller for longitudinal control of a high performance fighter using decoupling approach, the result is compared with the H_∞ method [7]. The authors proposed an blended autopilot for a missile with reaction-jet and aerodynamic fin [2]. Kim proposed the MIMO controller of hot rolling mill with decoupling compensator, the performance compared with the old conventional design is confirmed by the numerical simulations [3].

In this paper, the basic formulation of CDM is summarised in section 2. The lateral dynamics of an UAV is formulated in section 3, and the controller is designed in section 4. The performance of the system is evaluated by the numerical simulations in section 5.

2 Formulation based on CDM

The plant and controller are defined as follows in CDM.

$$\begin{aligned}&\text{Plant:} && \begin{cases} A_p(s)x = B_u(s)(u+d) \\ y = B_p(s)x \end{cases} \\ &\text{Controller:} && A_c(s)u = B_a(s)y_r - B_c(s)(y+n)\end{aligned} \tag{1}$$

Where, the states vector x, the outputs vector y, the reference input vector y_r, the control inputs vector u, the disturbance vector d, the noise input vector n are used.

Standard block diagram of the CDM design is shown in Fig. 1.

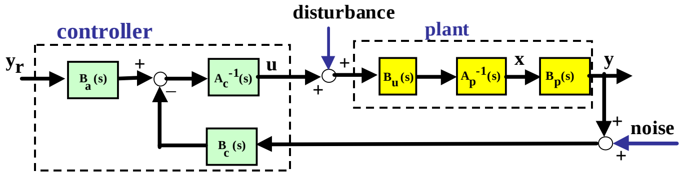

Fig. 1 Block diagram of control system

The closed loop system polynomial matrix is defined as,

$$A(s) = A_c(s)A_p(s) + B_c(s)B_p(s) \tag{2}$$

The characteristic polynomial $P(s)$ is defined as,

$$P(s) = ||A(s)|| = a_n s^n + \ldots + a_1 s + a_0 = \sum_{l=0}^{n} a_l s^l \tag{3}$$

The stability index γ_i and the time constant τ are utilised as design parameters in CDM and defined as,

$$\gamma_i = \frac{a_i^2}{a_{i+1}a_{i-1}} \quad (i = 1, \ldots, n-1) \tag{4}$$

$$\tau = a_1/a_0 \tag{5}$$

a_i is plotted in the coefficient diagram as shown in Fig. 2. The stability index is represented as convexity and the time constant is represented as slope in the diagram. The lower bound of stability index γ_i^* is defined as,

$$\gamma_i^* = 1/\gamma_{i+1} + 1/\gamma_{i-1} \quad (\gamma_0 = \gamma_n = \infty) \tag{6}$$

The sufficient condition for the stability [4] is given as,

$$\gamma_i > 1.12\gamma_i^* \quad (i = 1, \ldots, n-2) \tag{7}$$

By the use of Eqs.(4,5), the coefficient a_i is expressed by τ , a_0 and γ_i.

$$a_i = a_0 \frac{\tau^i}{\gamma_{i-1}\gamma_{i-2}^2 \cdots \gamma_2^{i-2}\gamma_1^{i-1}} \tag{8}$$

In the CDM, following stability indices are recommended [8].

$$\gamma_1 = 2.5, \gamma_2 = \ldots = \gamma_{n-1} = 2 \tag{9}$$

In this case, the step response has no overshoot, and the settling time is about 2.5...3τ [8].

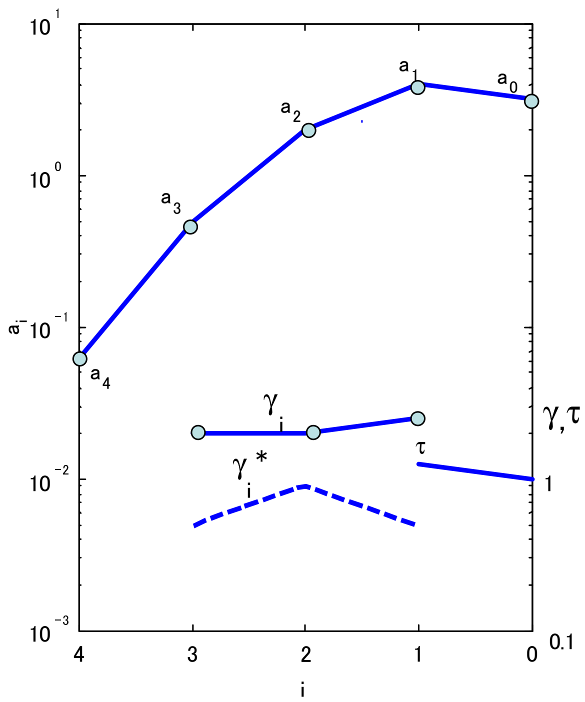

Fig. 2 A sample of coefficient diagram

3 Lateral dynamics of UAV

The lateral dynamics of UAV is represented as linear system by side-slip angle β , roll rate p, yaw rate r, bank angle ϕ. The control input variables are aileron δ_a and rudder δ_r. The requirements are to follow the bank command and to suppress excessive side-slip angle in the turning.

$$x = \begin{bmatrix} \beta & p & r & \phi \end{bmatrix}, u = \begin{bmatrix} \delta_a & \delta_r \end{bmatrix} \tag{10}$$

$$y = \begin{bmatrix} \beta & p & r & \phi \end{bmatrix}, y_r = \begin{bmatrix} \beta_c & \phi_c \end{bmatrix} \tag{11}$$

The system is represented as,

$$A_p = \begin{bmatrix} s - Y_\beta & -\sin\alpha_0 & \cos\alpha_0 & \frac{g\cos\alpha_0}{V_0} \\ -L_\beta & s - L_p & -L_r & 0 \\ -N_\beta & -N_p & s - N_r & 0 \\ 0 & -1 & -\tan\alpha_0 & s \end{bmatrix} \tag{12}$$

$$B_u = \begin{bmatrix} Y_{\delta_a} & Y_{\delta_r} \\ L_{\delta_a} & L_{\delta_r} \\ N_{\delta_a} & N_{\delta_r} \\ 0 & 0 \end{bmatrix} \tag{13}$$

The dynamics of fin actuators are defined as the first order lag as follows,

$$\frac{\delta_a}{\delta_{ac}} = \frac{1}{s/30+1}, \quad \frac{\delta_r}{\delta_{rc}} = \frac{1}{s/30+1} \tag{14}$$

4 Controller design

4.1 Characteristics of the plant

The aerodynamics parameters of an UAV [5] are used in this design. The design is performed in velocity 25m/s, altitude 500m. The steady state flight condition is assumed, and the angle of attack in steady state α_0 is 2.95deg. The aerodynamic coefficients in this condition are defined as in Tab. 1.

Table 1 aerodynamic coefficients

Y_{δ_a}	-0.0574	Y_{δ_r}	0.1465
L_{δ_a}	-126.0	L_{δ_r}	2.267
N_{δ_a}	-4.968	N_{δ_r}	-23.146
Y_β	-0.6711	L_p	-21.77
L_β	-110.56	L_r	10.48
N_β	17.94	N_p	-2.82
N_r	-1.095		

The pseudo control input u^* is defined for decoupling between yaw and roll channel.

$$E_1 u^* = u, \; E_1 = \begin{bmatrix} L_{\delta_a} & L_{\delta_r} \\ N_{\delta_a} & N_{\delta_r} \end{bmatrix}^{-1} \tag{15}$$

$$A_p(s)x = B_u u = B_u E_1 u^* = B_u^* u^* \tag{16}$$

$$B_u^*(s) = \begin{bmatrix} 0.0007 & -0.006 \\ 1 & 0 \\ 0 & 1 \\ 0 & 0 \end{bmatrix} \tag{17}$$

By the use of Eq.(1), the transfer function is defined as,

$$B_p^* = \begin{bmatrix} b_{11}(s) & b_{12}(s) \\ b_{21}(s) & b_{22}(s) \\ b_{31}(s) & b_{32}(s) \\ b_{41}(s) & b_{42}(s) \end{bmatrix} \tag{18}$$

$$y = \frac{1}{a_p(s)} B_p^* u^* \tag{19}$$

$$a_p(s) = ||A_p(s)||(s/30+1) \tag{20}$$

The denominator and numerator of transfer function are shown in Fig. 3. The negative coefficients are indicated by the sign (-). A negative coefficient of denominator indicates unstable spiral mode. The order of controller should be minimised to realize the simple on-board controller. The structure design of feedback controller is performed using this diagram.

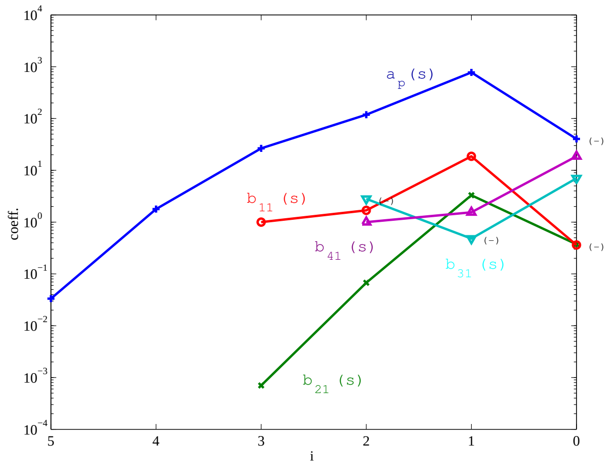

(a) aileron channel

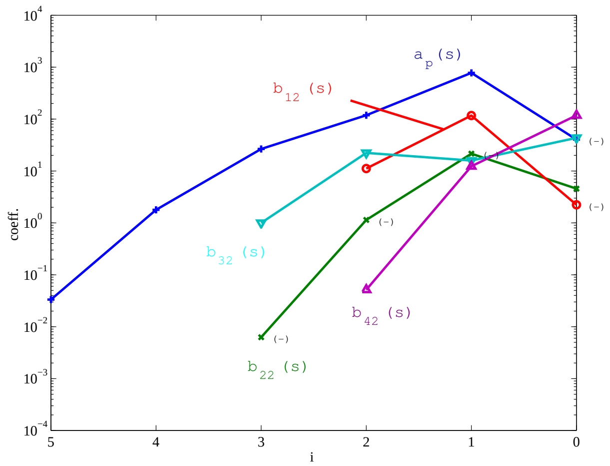

(b) rudder channel

Fig. 3 Coefficient diagram of lateral dynamics

4.2 Yaw channel controller

In the yaw channel, the proportional plus integral feedback of side-slip angle β and yaw rate r

are used as feedback signal. The control input is the pseudo rudder angle δ_r^*. The first order coefficient of $b_{12}(s)$ has the large value. Whereas, the first and second order coefficient of b_{32} has almost the same value, and the zeroth order coefficient has negative value of nearly the same magnitude.

The design process on CDM is to find the best combination of the feedback signal to compose the reference coefficient $P(s)$ defined in Eq.(3). The feedback signal having the large negative value is not preferable to maintain the robustness. From this consideration, the proportional and integral feedback of beta and proportional feedback of yaw rate are selected as feedback signal.

The controller and the system of the yaw channel are defined as,

$$B_p(s) = \begin{bmatrix} b_{12}(s) \\ b_{32}(s) \end{bmatrix}, \; A_p(s) = a_p(s) \tag{21}$$

$$B_c(s) = \begin{bmatrix} k_2 s + k_1 & k_0 s \end{bmatrix}, \; A_c(s) = s \tag{22}$$

$$B_a(s) = m_0 \tag{23}$$

The reference coefficients are defined as $P(s)$ of Fig. 4 based on the recommended form of CDM in Eq.(8), and the feedback gain to realise these coefficients are calculated as,

$$k_0 = 17.26, \; k_1 = -656.8, \; k_2 = -115.2$$
$$m_0 = 4210$$

The coefficients of feedback signals are also shown in the same figure. In the coefficient diagram of Fig. 4, the characteristic polynomial $P(s)$ is defined as the summation of the feedback signal as follows,

$$P(s) = sa_p(s) + k_2 s b_{12}(s) + k_1 b_{12}(s) + k_0 b_{32}(s) \tag{24}$$

The effectiveness and contribution of the each feedback signal are easily understandable by the coefficient diagram.

Although $P(s)$ has the negative coefficient of the zeroth order and the slow unstable spiral mode is still existing, it is easily compensated in the roll channel shown in the next section.

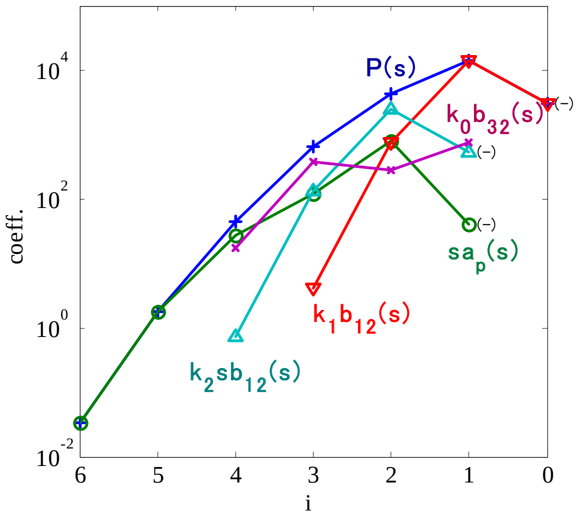

Fig. 4 Coefficient diagram of yaw channel

4.3 Roll channel controller

The first order coefficient of $b_{21}(s)$ which is also the zeroth order coefficient of $b_{41}(s)$ has large value. The first order coefficient of denominator $a_p(s)$ has also large value. Considering these characteristics, the integral feedback of bank angle and the integral feedback of roll rate are selected. the roll rate feedback is not effective because the second order coefficient already has the large value.

The controller and the system of the roll channel are defined as,

$$B_p(s) = \begin{bmatrix} b_{21}(s) \\ b_{41}(s) \end{bmatrix}, \; A_p(s) = a_p(s) \tag{25}$$

$$B_c(s) = \begin{bmatrix} k_4 & k_3 \end{bmatrix}, \; A_c(s) = s \tag{26}$$

$$B_a(s) = m_1 \tag{27}$$

The feedback gain are derived in the same manner as yaw channel.

$$k_3 = 137.2, \; k_4 = 135.0, \; m_1 = 134.6$$

The coefficients of transfer functions are shown in Fig. 5. The time constant τ is selected as 1.07.

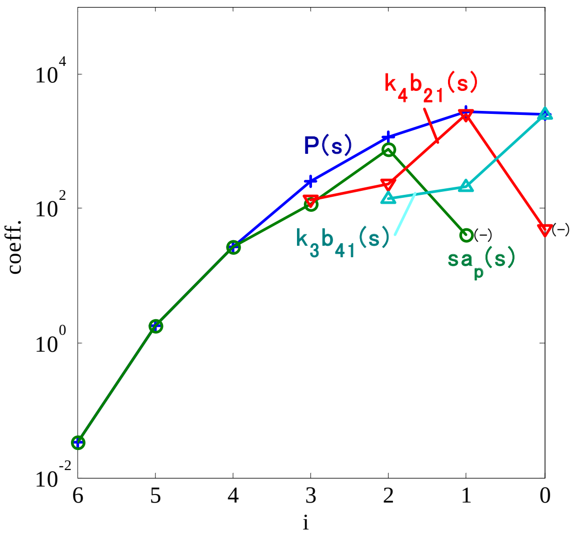

Fig. 5 Coefficient diagram of roll channel

4.4 Cross-feed compensation and total system

The inter-channel cross-feed compensation k_5 is introduced to compensate the kinematic coupling term $p\sin\alpha$ on the side slip dynamics. k_5 is selected as 2.5 for proper time response.

The controller of the total system is defined as,

$$B_c(s) = \begin{bmatrix} 0 & k_4 & 0 & k_3 \\ k_2 s + k_1 & k_5 & k_0 s & 0 \end{bmatrix} \quad (28)$$

$$A_c(s) = \begin{bmatrix} s & 0 \\ 0 & s \end{bmatrix} \quad (29)$$

$$B_a(s) = \begin{bmatrix} m_1 & 0 \\ 0 & m_0 \end{bmatrix} \quad (30)$$

5 Design confirmation by the numerical simulations

Some nonlinear 6DOF simulations [10] are performed to confirm the performance of the control system. The step response of 45 degrees bank command is shown in Fig. 6. To evaluate the effectiveness of the cross-feed compensation, the result without the cross-feed compensation ($k_5 = 0$) is also shown in the same figure. The maximum side slip angle in the transient is small and lower than 1 degree. The transient response is improved by the cross-feed compensation. The bank response has no overshoot and its settling time is about 3τ.

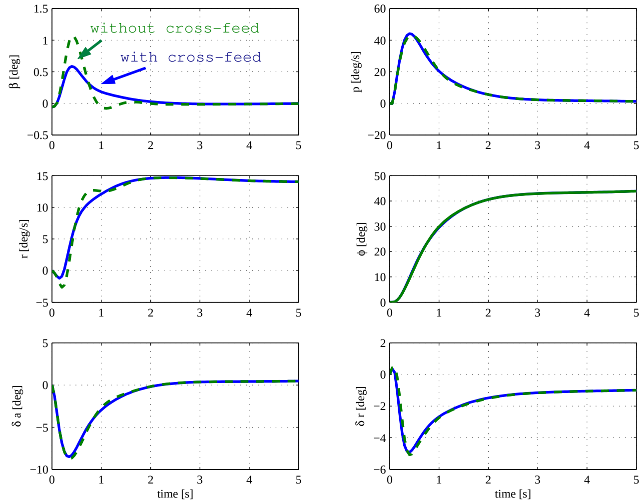

Fig. 6 6DOF simulation of roll step response

6 Conclusion

The MIMO lateral autopilot for an UAV is designed using CDM. The control inputs are decoupled by introducing the pseudo-control input. The yaw and roll channel controller is separately designed for the decoupled system. The interference between yaw and roll channel is compensated by the cross-feed compensator. The controllers are successfully designed by CDM and the performance is confirmed by six-degrees-of-freedom (6DOF) simulation.

Acknowledgements

The authors would like to thank Shunji Manabe for his extensive support for this research.

References

[1] A.Ucar and S.E.Hamamci. Controller based on coefficient diagram method for the robotic manipulators. In *The 7th IEEE International Conference on Electronics, Circuits and Systems*, pages 777–780, Kaslik, Lebanon, December 2000.

[2] Rui Hirokawa, Koichi Sato, and Shunji Manabe. Autopilot design for a missile with reaction-jet using coefficient diagram method. In *Proceedings of AIAA Guidance, Navigation, and Control Conference*, number AIAA 2001-4162, Montreal, Canada, August 2001.

[3] Young-Chol Kim and Myung-Joon Hur. Application of CDM to MIMO systems: Control of hot rolling mill. In *ICASE: The Institute of Control, Automation and Systems Engineers*, volume 3, pages 250–256, Korea, December 2001.

[4] A. V. Lipatov and N.I.Sokolov. Some sufficient conditions for stability and instability of continuous linear stationay systems. *Automatic Remote Control*, pages 1285–1291, 1979. translated from Automatika i Telemekhanika, No.9,pp. 30–37, 1978.

[5] Aerosonde Ltd. The aerosonde system. Notting Hill, Australia.

[6] S. Manabe. Coefficient diagram method as applied to the attitude control of controlled-bias-momentum satellite. In *13 th IFAC Symposium on Automatic Control in Aerospace*, pages 322–327, Sept 1994.

[7] S. Manabe. Application of coefficient diagram method to mimo system. In *10 th Workshop on Astrodynamics and Flight Mechanics*. ISAS, July 2000.

[8] Sunji Manabe. The coefficient diagram method. In *14 th IFAC Symposium on Automatic Control in Aerospace*, Seoul, Korea, August 1998.

[9] Sunji Manabe. Comparison of h-inf and coefficient diagram method in aerospace. In *Proceedings of 19th Guidance Control Symposium*, Yokohama,Japan, November 2002.

[10] Unmanned Dynamics, Hood River OR. *AeroSim User's Guide*, 2002.